JACS
JOURNAL OF THE AMERICAN CHEMICAL SOCIETY
Article
pubs.acs.org/JACS

Description of Hydration Water in Protein (Green Fluorescent Protein) Solution

Stefania Perticaroli,[*,†,§,¶] Georg Ehlers,[‡] Christopher B. Stanley,[§] Eugene Mamontov,[∥] Hugh O'Neill,[§,#] Qiu Zhang,[§] Xiaolin Cheng,[⊥,#] Dean A. A. Myles,[§] John Katsaras,[†,§,▽] and Jonathan D. Nickels[*,†,§,▽,¶]

[†]Shull Wollan Center, a Joint Institute for Neutron Sciences, [‡]Quantum Condensed Matter Division, [§]Biology and Soft Matter Division, [∥]Chemical and Engineering Materials Division, and [⊥]Center for Molecular Biophysics, Oak Ridge National Laboratory, Oak Ridge, Tennessee 37831, United States

[#]Department of Biochemistry and Cellular and Molecular Biology and [▽]Department of Physics and Astronomy, University of Tennessee, Knoxville, Tennessee 37996, United States

Supporting Information

ABSTRACT: The structurally and dynamically perturbed hydration shells that surround proteins and biomolecules have a substantial influence upon their function and stability. This makes the extent and degree of water perturbation of practical interest for general biological study and industrial formulation. We present an experimental description of the dynamical perturbation of hydration water around green fluorescent protein in solution. Less than two shells (~5.5 Å) were perturbed, with dynamics a factor of 2−10 times slower than bulk water, depending on their distance from the protein surface and the probe length of the measurement. This dependence on probe length demonstrates that hydration water undergoes subdiffusive motions ($\tau \propto q^{-2.5}$ for the first hydration shell, $\tau \propto q^{-2.3}$ for perturbed water in the second shell), an important difference with neat water, which demonstrates diffusive behavior ($\tau \propto q^{-2}$). These results help clarify the seemingly conflicting range of values reported for hydration water retardation as a logical consequence of the different length scales probed by the analytical techniques used.

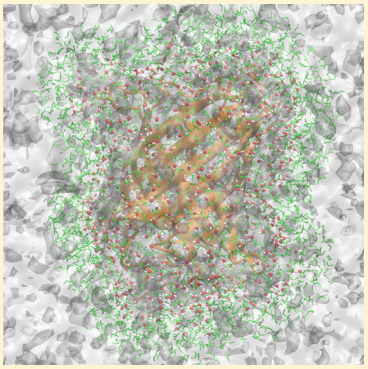

INTRODUCTION

The term "hydration water" describes the structurally and dynamically perturbed water surrounding proteins and biomolecules. This population of water has a defining influence on the structure and function of biomolecules,[1,2] especially proteins;[3] implying a fundamental connection between the dynamical properties of hydration water and many vital biochemical processes including protein folding, protein−ligand recognition, membrane, enzyme function, and DNA stability.[4−8] In the food, cosmetics, and pharmaceutical industries,[6,9] hydration water impacts properties such as solubility, emulsification, foamability, viscosity, gelation, and degradation.[9] Despite this obvious importance, a robust description of the hydration population of water has been challenging. Certainly, part of this derives from the heterogeneity of the hydration shell at a molecular scale. Topological disorder of the biomolecule surface and the chemical heterogeneity of the solvent-exposed groups result in a diverse molecular environment, with hydration water exhibiting different dynamics[10−24] relative to neat water. The way that these effects manifest in various experimental techniques can lead to discrepancies based on the time and length scales inherent in the measurements and property that is probed.[25]

Two parameters are typically used to describe the extent and magnitude of this perturbation: the hydration number, N_H, and the retardation factor, ξ. N_H describes the extent of the perturbation in terms of the number of water molecules surrounding the protein whose physical properties are altered, as defined by a specific technique or analysis. ξ quantifies the magnitude of the perturbation as the ratio of characteristic relaxation times for hydration water relative to bulk, τ_{HYDR}/τ_{BULK}. This has the advantage of being less dependent on the specific correlation functions analyzed than reporting the absolute values of τ obtained from a specific technique. However, there are discrepancies in the literature about the magnitude of ξ, with results from NMR[12,22] and MD simulations[13,23,26] suggesting a slowdown of 2−5 times in the first hydration shell, while time-resolved fluorescence spectroscopy[5,17,27] reports a significant proportion of the water population being slowed by 1−2 orders of magnitude.

Neutron scattering (NS) spectroscopy is a two-dimensional technique that provides information about atomic motions in both time and space, with accessible length scales from angstroms to nanometers; with broad dynamic ranges from hundreds of nanoseconds to femtoseconds that can be accessed by combining spectra from more than one instrument. Moreover, due to the large incoherent scattering cross section of hydrogen (H), larger than its isotope deuterium (D) or other elements (C, O, N, S), NS provides the notable opportunity to distinguish the dynamics of the solvent from those of the protein, or vice versa, through isotopic sensitivity.

Received: August 23, 2016
Published: October 26, 2016

DOI: 10.1021/jacs.6b08845
J. Am. Chem. Soc. 2017, 139, 1098−1105

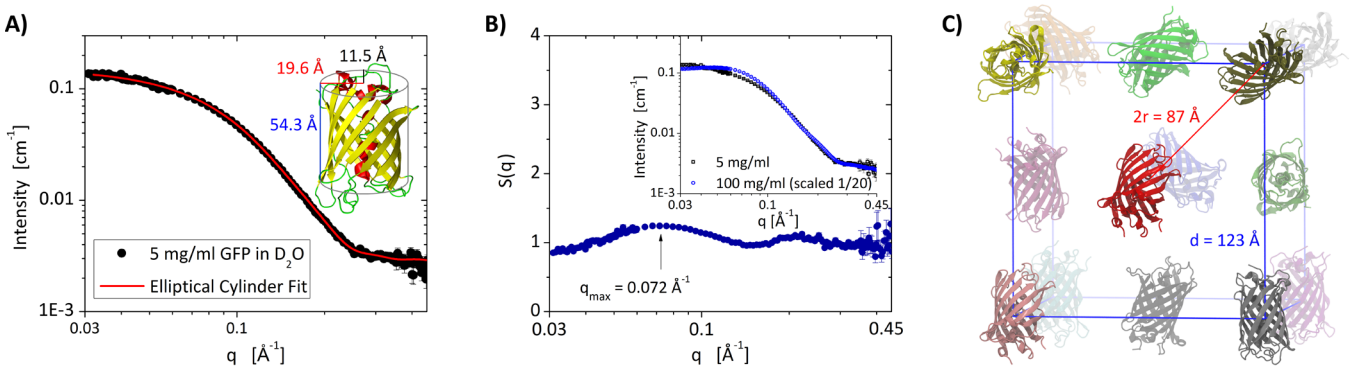

Figure 1. Small angle neutron scattering of GFP solutions. GFP solutions were prepared in D_2O and measured at 283 K. (A) Solution scattering from GFP at 5 mg/mL was found to be well modeled using an elliptical cylinder. An estimate of the molecular weight was made from the forward scattering (29.8 vs 27 kDa predicted from sequence). (B) Protein−protein correlations in the 100 mg/mL solution result in a structure factor typical of repulsive particles. (C) Due to the high aspect ratio of GFP, a hard sphere approximation does not accurately reproduce this structure factor. Therefore, an approximation is made taking q_{max} to be the nearest neighbor distance and the solution structure equated to a close packed FCC lattice, with GFP at the atom positions. This treatment models the data well and returns a volume fraction of 8.2% for GFP at 100 mg/mL in solution (equivalent to ∼98 mg/mL). (One chain from the 1GFL structure was used in creating these figures.)

This makes NS ideal to study water diffusion, rotation, collective motions, and other interatomic interactions.[28] Importantly, the characteristic time scale of the probed single molecule translational−rotational dynamics is fast in comparison to the residence time of the water molecules within the shell. This means that the slow exchange condition[29] is met and the two populations of water (hydration and bulk) can be distinguished. In this way, NS experiments provide simultaneous estimates of N_H and ξ at a range of experimental probe lengths, revealing the underlying relationship between the probe distance and the observed ξ.

In this work, we study hydration water in a 100 mg/mL solution of green fluorescent protein (GFP). This concentration was chosen for its biological and biotechnological relevance. Total concentrations of up to 400 mg/mL have been reported in cellular compartments, perturbing water motions.[30,31] Similarly high protein concentrations, up to or greater than 100 mg/mL, are also found in therapeutic formulations, such as for monoclonal antibodies, due to high dosage (∼100 mg) therapies and the volume limit (<1.5 mL) of subcutaneous injections.[32] GFP itself is a widely used probe in molecular and cell biology;[33] typically deployed as a fusion protein, it often serves to track expression, localization, and motion of other molecules. Here, it serves as a model protein around which we can measure the translational−rotational dynamics of hydration water using NS.

NS allows us to construct an experimental description of hydration water around GFP, and by explicitly measuring the dynamics as a function of length scale, we can observe how the length scale of a measurement impacts the quantities N_H and ξ. We found that less than two full shells of water are perturbed by GFP, with the first shell showing greater perturbation than water molecules in the second shell. Moreover, retardation factors were found to strongly depend on the length scale of the observation, with ξ increasing as a function of probe length. In the first shell, ξ increased from 4 when a 3 Å probe length was used to 10 for a probe length of 13 Å. In the second shell, ξ rose from 2 at a 3 Å probe length to 5 when probed over 13 Å. We conclude that this dependence has a physical origin in the comparison of the subdiffusive motions of hydration water ($\tau \propto q^{-2.5}$ for the first and $\tau \propto q^{-2.3}$ for the perturbed water molecules in the second shell) with the diffusive motions ($\tau \propto q^{-2}$) of bulk water. This demonstrates the inherent importance of the experimental probe length when comparing these two water populations.

RESULTS

GFP solutions were first characterized with small angle neutron scattering (SANS). Measurements of 5 and 100 mg/mL solutions of H-GFP in D_2O were carried out at EQ-SANS[34] at the Spallation Neutron Source, Oak Ridge National Laboratory (Tennessee, USA), over a q-range of 0.03−0.45 Å^{-1} (Figure 1). Full details of sample preparation and experimental conditions are reported in the Materials and Methods section in Supporting Information. Using the forward scattering, I_0, we estimated molecular weight (MW) to be 29.8 kDa, indicating that GFP is monomeric in solution at 5 mg/mL concentration (MW is predicted to be 27 kDa from the sequence), consistent with recently published SAXS and SANS measurements.[35] Details of this calculation can be found in Supporting Information. The shape of the protein in solution was fit to an elliptical cylinder model. Fitting was performed in the SASview suite[36] using the DREAM algorithm (Figure 1A), providing a good fit to an elliptical cylinder with a height of 54.3 ± 1.3 Å with a major radius of 19.6 ± 2.0 Å and a minor radius of 11.5 ± 0.6 Å (χ^2 < 1.5, fit details in Figure S1 in Supporting Information).

SANS data for GFP at 100 mg/mL were used to obtain the structure factor. This was calculated by scaling the 100 mg/mL data by 1/20 and dividing it by the 5 mg/mL data (Figure 1B). The resulting structure factor exhibits the typical shape of repulsive particles in solution. Due to the shape of GFP (high aspect ratio), the data is not well fit by a hard sphere approximation. Therefore, the data is analyzed using the first peak maximum, q_{max} = 0.072 Å^{-1}, as the average spacing, $2r$ = 87.2 Å, to the next nearest GFP molecule in solution, $2r = 2\pi/q_{max}$. We then combine this with an approximation of the relative spacing of GFP molecules in solution. The center of mass of GFP was placed at the atom positions of a face centered cubic lattice to represent close packing in solution (Figure 1C). In this model, the edge length of the "unit cell" is given by $d = 2r\sqrt{2}$, or d = 123.4 Å, resulting in a "unit cell" volume $V_{FCC} = 1.87 \times 10^6$ Å^3. Taking the volume of GFP from the shape analysis above, 3.82×10^4 Å^3, and recalling that there

DOI: 10.1021/jacs.6b08845
J. Am. Chem. Soc. 2017, 139, 1098−1105

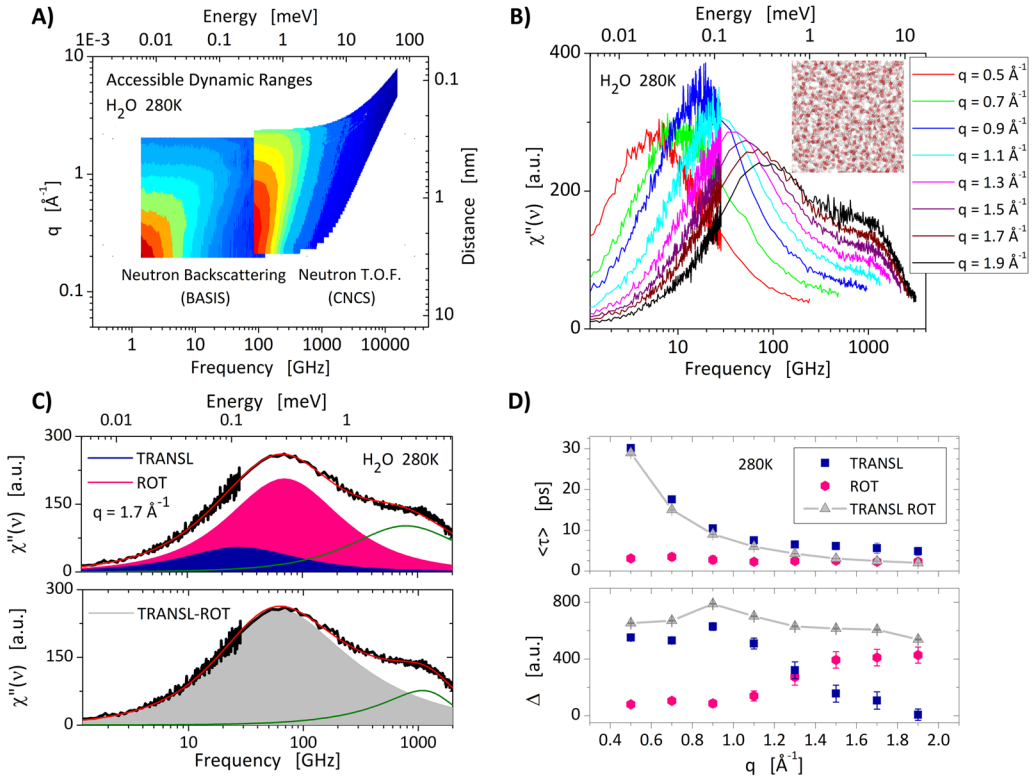

Figure 2. Water dynamics. (A) Experimental NS spectra of pure H_2O at 280 K, registered on the BASIS and CNCS instruments. The spectra show scattered intensity as a two-dimensional function of energy transfer (bottom axis) and wave vector (left axis); these properties can be equated to frequency (right axis) and probe length (top axis). Intensity is shown as a color mapping scaled from blue to red. (B) Stitched spectra of H_2O. Spectra are evaluated at eight different q values and stitched to provide a dynamical range of up to three decades. Spectra were normalized on the sample mass in the beam. (C) Two methods to fit the water spectra (black line): upper panel, fit with 2 Debye functions for translational (blue area) and rotational (pink area) dynamics; lower panel, fit with a CD function accounting for coupled translational−rotational dynamics (gray area). In both graphs, the DHO function representing the collective modes of hydrogen bond bending is depicted in green and the total fit in red. (D) Comparison of fit parameters. The average relaxation time of the single CD component is similar to τ_{TRANSL} at low q and to τ_{ROT} at high q obtained with the decoupling assumption. Amplitudes, Δ, of the CD fit match the sum of amplitudes of the two Debye functions.

would be an average of four proteins in that FCC "unit cell", we can estimate a volume fraction, f_{GFP}, of 8.2% for the 100 mg/mL solution. As a check, we can now calculate the mass fraction of GFP in this solution by converting through the density of protein, 1.35 g/mL, and D_2O, 1.11 g/mL, to arrive at 9.8% (or 98 mg/mL), very reasonable for a solution prepared at 100 mg/mL.

With this structural information in hand, we can move to the dynamical description of the hydration water surrounding the protein. We must first measure neat water at 280 and 303 K for comparison. Dynamics data were collected on two NS spectrometers, BASIS[37] and CNCS,[38] at the Spallation Neutron Source, Oak Ridge National Laboratory, Tennessee, USA. These spectrometers measure scattered intensity (dynamical structure factor), $S(q,E)$, in an overlapping range (Figure 2A), where E is energy transfer and q is momentum transfer. The experimental spectra were first processed into slices along the energy axis, binning the data at defined q-values common to both instruments, and then transformed into the susceptibility formalism, $\chi''(q,\nu)$ according to the relation; $\chi''(q,\nu) \propto S(q,\nu)/n_B(\nu)$, where $S(q,\nu)$ is the measured dynamic structure factor and $n_B(\nu) = [\exp(h\nu/(kT)) - 1]^{-1}$ is the Bose occupation number.[28] Though neutron data is widely analyzed in intensity, the susceptibility representation is also commonly used[39−41] and has the advantage that the inelastic/quasielastic regions of the spectra are emphasized. This presentation can also be directly compared to other techniques. Moreover, well separated processes appear as distinct maxima.[42] This is especially useful when partially overlapping data from two spectrometers can be stitched together at common q-values, similar to the procedure used in extended depolarized light scattering (EDLS) experiments.[18,19] We find the susceptibility formalism to be an insightful and useful presentation of the dynamics data in this case, covering up to three decades in frequency, ν, for probe lengths of ∼3 Å to 1.3 nm. This is shown for neat water at 280 K in Figure 2B.

Typically, NS spectra from each instrument are modeled independently using Lorentzian functions in the intensity formalism (equivalent to Debye functions in susceptibility). Because of this, many authors have faced difficulties in resolving the processes contributing to the spectra of neat water, invoking a number of models such as the jump diffusion model, relaxing cage model, and others. It is important to note that these samples are hydrogen rich molecules (H_2O and protein), meaning that we overwhelmingly observe incoherent scattering, reflecting the self-correlation functions of hydrogen atoms in the sample.[28] Careful analysis by Teixeira and co-workers established the presence of translational and rotational contributions in the NS spectra of neat water,[43] with translational dynamics dominating at low q (large probe distance) and rotational motions prevailing at high q (short probe distance). There are also phonon-like collective vibra-

DOI: 10.1021/jacs.6b08845
J. Am. Chem. Soc. 2017, 139, 1098−1105

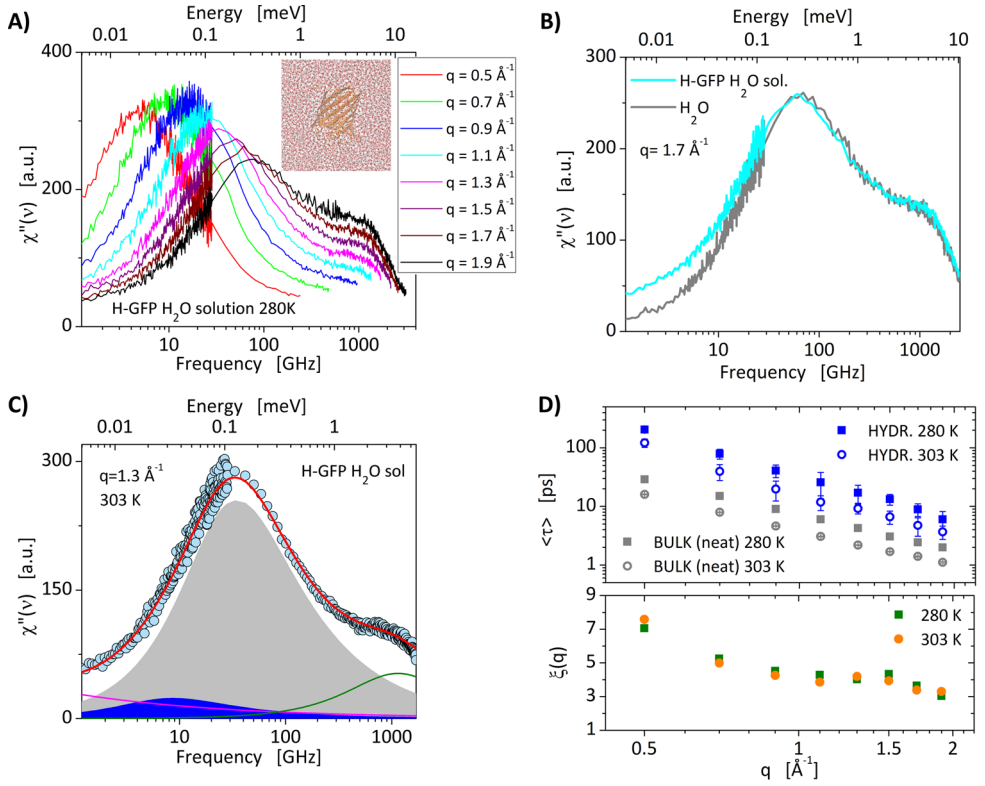

Figure 3. Hydration water dynamics in GFP solution. (A) NS spectra of H-GFP H_2O 100 mg/mL solution for eight q-values; data were normalized to the sample mass. The signal is dominated by the solvent contribution. Spectra of H_2O and H-GFP H_2O solution at 303 K are reported in Figure S4. (B) Comparison between the spectra of neat H_2O (gray) and H-GFP H_2O solution (cyan) at same q (1.7 $Å^{-1}$) and temperature (280 K). (C) Typical fit of a spectrum (circles) of H-GFP H_2O solution (q = 1.3 $Å^{-1}$, 303 K). Relaxation processes of hydration and bulk water are shown in blue and gray, respectively (CD functions). Power law representing protein motions appears in magenta, DHO for protein and water vibrations appears in green, and the total fit is shown in red. (D) upper panel, average relaxation times of hydration (blue symbols) and bulk (gray) water obtained from the fit at 280 (squares) and 303 K (circles) as a function of q; lower panel, q dependence of the retardation factors for the total perturbed water population at 280 (green squares) and 303 K (orange circles).

tional motions present at ~6 meV (1500 GHz) for q > 0.4 $Å^{-1}$.[44−48] This treatment, which assumes decoupling between translational and rotational motions of water, was introduced because it leads to a tractable analytical model for the scattering function,[43] rather than providing the most realistic description of the water dynamics at a molecular level. In fact, it is known that translational and rotational motions of bulk water are indeed weakly coupled at low q (≤1 $Å^{-1}$) and strongly correlated at high q (>1 $Å^{-1}$) (at 280 K and room temperature).[49,50]

It is therefore reasonable to model the same data of neat water using a single functional form, a Cole−Davidson (CD) function, $\chi''_{CD} = -\mathcal{I}m\{\Delta_{CD}[1 + i\omega\tau_{CD}]^{-\beta}\}$, with a stretching exponent β = 0.7, where Δ_{CD} is the amplitude and τ_{CD} is the relaxation time describing the coupled translational−rotational dynamics. In Figure 2C, we show how both approaches can reproduce the spectra for neat water. In the upper panel, the data is treated with two Debye functional forms, representing the translational and rotational contributions of water, with a damped harmonic oscillator (DHO) accounting for the intermolecular collective modes of H-bond bending motions at ~1500 GHz.[18,19,21] The DHO is given by the relation $\chi''_{DHO} = \mathcal{I}m\{\Delta_{DHO}{\omega_0}^2[\omega^2 - {\omega_0}^2 - i\omega\Gamma_{CD}]^{-1}\}$, where ω_0 is the position, Γ is the width, and Δ_{DHO} is the amplitude. This fit shows close agreement with literature data[43] (Figure S3), with the translational relaxation times decreasing in q, while τ_{ROT} remains constant (Figure 2D, upper panel). The lower panel shows the fit of the same spectra using a Cole−Davidson (CD) function and a DHO form for the collective H-bond bending. The amplitude of the CD component closely resembles the sum of the two Debye functions from the decoupled fit where the translational contribution dominates at low q and the rotational component at high q (Figure 2D, lower panel). This CD fitting approach has the advantage of reflecting the coupled nature of water motions on these time and length scales, as well as reducing the number of fit parameters. This point is particularly useful when considering the treatment of two separate water populations (bulk and hydration) in subsequent analyses of hydration water.

H-GFP solution at 100 mg/mL in H_2O was measured at 280 and 303 K on both BASIS and CNCS. The data were processed as described above for neat water, yielding the stitched spectra shown in Figure 3A. The spectra for both neat water and the H-GFP H_2O solution at 303 K can be found in the Supporting Information. It is clear that the solvent contribution dominates these spectra, with 93.9% of the total scattering cross-section of the samples coming from H_2O (Table S1). However, the solution spectra do show increased intensity at low frequency when compared to neat water (Figure 3B). This intensity comes from motions of the protein and the slower water population in the hydration shells, which have been perturbed by the protein. We introduce an additional CD function to model hydration water, allowing both τ and amplitude to float.

DOI: 10.1021/jacs.6b08845
J. Am. Chem. Soc. 2017, 139, 1098−1105

A CD function with variable amplitude and τ_{BULK} fixed to that of neat water was used to account for bulk water. β was fixed at 0.7 for both CD functions. The dynamics of the protein at low frequencies were reproduced by a $\nu^{-0.3}$ power law.[18,42,51] This contribution is not analyzed further, though a characterization of GFP dynamics can be found in the literature,[16,52−56] in addition to studies focused on the contribution from the global motions of proteins in solution.[57,58] We note that global protein motions are more appropriately studied in D_2O solutions[57,58] or with neutron spin−echo spectroscopy.[59] These and other approaches, such as NMR and DLS, are also used to investigate crowded protein solutions.[60,61] At high frequency, the spectra for neat water and H-GFP H_2O solution overlap (Figure 3B). Contributions from the protein collective motions[18,62,63] at high frequency were not detectable, and the collective vibrational motions of hydration water are similar to those of neat water in this q-range.[44−46,48,64] This fit was carried out at all eight values of q for data collected at 280 and 303 K. A representative fit of the solution spectra is shown in Figure 3C.

Relaxation times, τ, for hydration and bulk water are reported in Figure 3D (upper) as a function of q. It is immediately clear that hydration water motions are slower than water in the bulk. Also, while neat water shows typical diffusive motions with $\tau \propto q^{-2}$, hydration water shows a $\tau \propto q^{-2.4}$ dependence (on average), indicative of subdiffusive motions. This difference is clear when we analyze the magnitude of the slowdown in water as the retardation factor, $\xi(q)$, Figure 3D (lower). ξ is consistent at both temperatures and shows a clear q-dependence, decreasing from ∼8 at q = 0.5 Å^{-1} to ∼2 at q = 1.9 Å^{-1}. This result is consistent with MD simulations obtained by Marchi et al.[14] who showed that the rotational relaxation of water in the vicinity of lysozyme is 3−7 times slower than that in the bulk depending on how the hydration shell (cutoff distance) is defined in the calculation, similar to our use of probe distance here. The amplitude of the two CD functions can be used to calculate the relative populations of hydration and bulk water according to the equation $N_H = \Delta_{HYDR}(\Delta_{HYDR} + \Delta_{BULK})^{-1}f^{-1}$, where Δ_{HYDR} and Δ_{BULK} are the amplitudes of hydration and bulk water contributions and f is the solute mole fraction. This calculation indicates that the translational−rotational dynamics of ∼1470 water molecules per protein are perturbed (∼10% of the total water). N_H does not show any significant variation in temperature and only a weak dependence on q in the explored range (Figure 4B).

To put this value of N_H in a geometric/structural context, analysis was carried out using an atomistic model of GFP in a box with 17 000 explicit water molecules. The model was equilibrated at 300 K for 20 ns (Figure 4A and Supporting Information) using NAMD 2.9[65] with the CHARMM C36 force field.[66] The number of water molecules in the first and second hydration shells was then computed, adopting the definition of Chen et al.[67] We declare a water molecule to be in the first shell if at least one of its hydrogens can be found within a 3.3 Å radius from a non-hydrogen atom of the protein, and to the second shell if it is located within a distance of 3.3 to 5.5 Å. This provides an estimate of ∼863 water molecules in the first shell and a total of 1706 within the first two shells. This estimate for the first hydration layer is in line with the simple calculation from the solvent accessible surface area, SASA, of GFP provided by the MD simulations, which gives ∼842 water molecules (details in the Supporting Information). The N_H result from analyzing the NS spectra of GFP solution, ∼1470 water molecules, therefore corresponds to slightly less than two

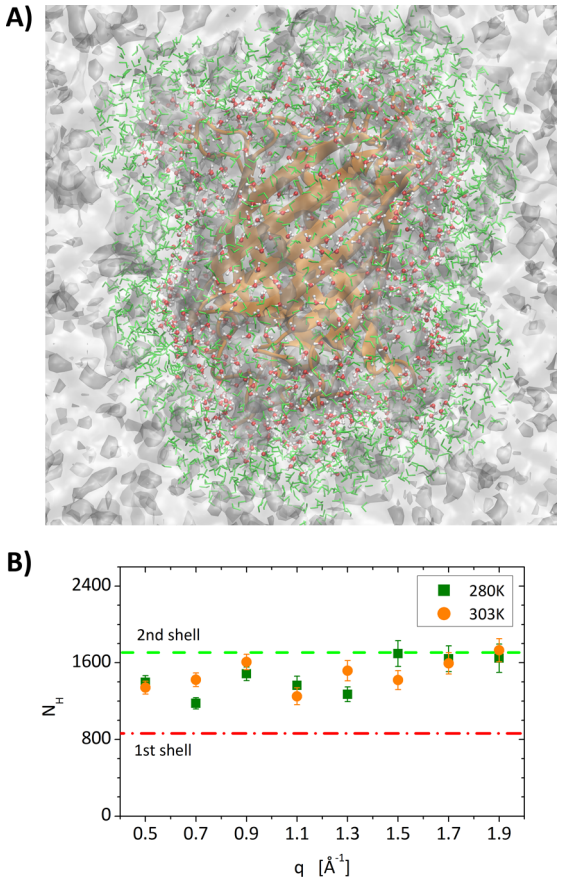

Figure 4. Hydration shells of GFP in H_2O. (A) The perturbation involves the first shell (red) and part of the second shell (green). (B) The hydration number estimated from the fit of H-GFP H_2O solution at 280 K (green squares) and 303 K (orange circles). Dashed lines correspond to the number of water molecules in the first shell (3.3 Å, red) and complete second shell (5.5 Å, green) estimated from simulation. Slightly less than two shells of water around were found to be perturbed.

full hydration shells. These hydration water molecules out to 5.5 Å from the protein surface would be expected to influence the diffusion coefficient of the protein, potentially impacting the experimentally determined hydrodynamic radius.

Simulations[68,69] suggest that the mobility of hydration water is strongly dependent on its distance from the protein interface, with an increase in mobility over the first 15 Å from the protein surface. We have investigated this experimentally, using an additional set of NS measurements on hydrated protein powders, H-GFP H_2O (h = 0.4 w/w) (Figure 5A). In this sample, the scattered intensity comes from the protein and the water absorbed on its surface. We assume that this models the motions of the protein and first hydration shell in solution,[2,21,42,70,71] an approach similar to what has been done for peptide/water solutions.[20] This assumption also relies on the functional argument that this level of hydration has been demonstrated to be sufficient for protein activity in powders[2,70,71] and is roughly equivalent to one shell. Data were collected at 280 K and processed as described above. Using these observations, we can reveal the contribution of perturbed water molecules in the second shell by noting that a linear combination (LC) of the powder and neat water spectra cannot reproduce that of the solution (scale factors reflect masses in the beam) (Figure 5C). Note that while the LC

DOI: 10.1021/jacs.6b08845
J. Am. Chem. Soc. 2017, 139, 1098−1105

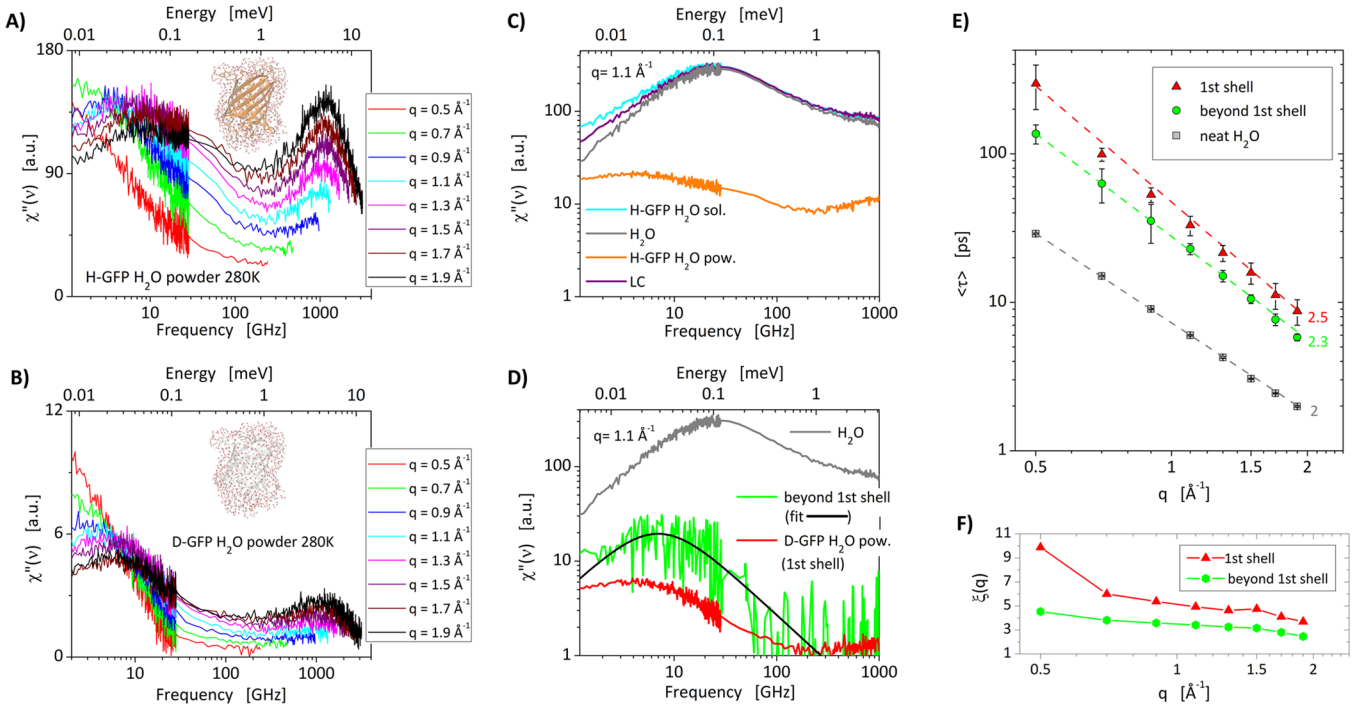

Figure 5. Resolving hydration water dynamics in the first and second shells. NS spectra of (A) H-GFP H_2O powder (h = 0.4) and (B) D-GFP H_2O powder (h = 0.4) at 280 K. Spectra normalized on the sample weight in the beam. (C) Spectrum of H-GFP H_2O solution (cyan) shown together with the linear combination (LC, purple) of the spectrum of neat water (scaled by a factor 0.93, gray) and H-GFP H_2O powder (scaled by a factor 0.07, orange), where the scaling factors correspond well to the amount of each component in solution (q = 1.1 $Å^{-1}$ and 280 K). At low frequency, the solution spectrum presents extra intensity relative to the LC. (D) The difference spectrum obtained by subtracting the LC profile from that of the solution represents the perturbed water beyond the 1st shell, which is shown in green (scaled up by a factor 2.5 to better visualize the shift in frequency relative to the other two water populations). This is compared to the motions of the 1st hydration shell, from D-GFP H_2O powder (red) and bulk water (gray) (q = 1.1 $Å^{-1}$ and 280 K) . The black line indicates the Debye fit used to extract the relaxation time of the perturbed water beyond the first shell. (E) Different q dependences of the relaxation times of bulk (neat) water ($\tau \propto q^{-2}$) (gray), first hydration shell ($\tau \propto q^{-2.5}$) (red), and perturbed water beyond the first shell ($\tau \propto q^{-2.3}$) (green). (F) Retardation factor ξ for water molecules of first and beyond first shell as a function of q.

reproduces the spectral profile of the solution at high frequency, there is excess intensity in the solution spectra below 50 GHz, Figure 5D. We assign this to the relaxation of perturbed water molecules beyond the first shell, showing the result of a Debye fit of this excess in Figure 5E.

To isolate the dynamics in the first shell, we invoke the greater scattering cross section of hydrogen relative to its stable isotope deuterium and analyze the NS spectra of perdeuterated GFP powder, hydrated with H_2O (D-GFP H_2O powder, h = 0.4) (Figure 5B).[16] We assume this data to represent the dynamics of water in the first hydration shell,[2,21,42,70,71] a minor contribution from exchangeable protons on the protein is present[21] though it is not typically treated explicitly.[11,16,72] These spectra can be fit directly and are shown in Figure 5E together with τ obtained for neat water and perturbed molecules beyond the first shell. The dynamics in both shells of hydration water are slower than bulk water, with first hydration shell slower than the perturbed water molecules in the second shell. The results, shown as a function of q, again show the clear difference between the diffusive q^2 dependence[73] of neat water and the subdiffusive dependence of hydration water, with $\tau \propto q^{-2.5}$ for the first hydration layer and $\tau \propto q^{-2.3}$ for the molecules perturbed in the second shell. Very similar q dependences have been found by NS investigations on hydration water surrounding C-phycocyanin ($q^{-2.44}$)[11,74] and phytoglycogen ($q^{-2.6}$)[15] and by MD studies on hydrated lysozyme ($q^{-2.5}$).[75] Protein surface roughness,[76] topological disorder, and electrostatic interactions are responsible for this diffusion dispersive regime.[77]

The values of ξ (Figure 5F) are consistent with the degree of slowdown observed with other techniques such as EDLS, NMR, and other MD simulations studies. For example, EDLS experiments found $\xi = 7 \pm 2$ for hydration water in lysozyme solutions,[18] while NMR studies have reported translational diffusion coefficients and reorientational correlation times of hydration water around proteins about 2−5 times slower than bulk.[12,22] The number of molecules involved is, however, more controversial. Time-resolved fluorescence spectroscopy and terahertz spectroscopy[5,17,27] suggest the presence of coupled water−protein picosecond fluctuations extending well beyond the first hydration shell up to 15−20 Å.[10] EDLS finds perturbations out to about 12 Å, while NMR operates in the fast exchange condition and has to fix the number of perturbed water molecules in order to estimate ξ.[29] MD simulations present a picture of moderate perturbation, mainly due to an excluded volume effect dependent on local surface topology.[23] Water reorientational and translational dynamics are reported to be slowed by a factor of 2−3 compared to bulk water[13,23,26] and effects extending to the second hydration shell only for the protein sites with a large charge density.[78] This is consistent with our findings of an incomplete perturbation of the second shell.

We wish to call attention to the systematic change in ξ as a function of q in the context of these discrepancies across

DOI: 10.1021/jacs.6b08845
J. Am. Chem. Soc. 2017, 139, 1098−1105

different techniques. Bulk water and hydration water motions are described by different power laws, diffusion versus subdiffusion. Because of this, hydration water dynamics appear more perturbed when probed over long distances (low q) than when probed at shorter distances (high q). This rationalizes the large perturbation observed with time-resolved fluorescence and terahertz spectroscopy, which are sensitive to long-range protein−water couplings, while NMR with its localized probe observes smaller perturbations in hydration water. This clearly makes the point that any measurement of water perturbation must be associated with the length scale(s) at which it was measured. The difference in q-dependence is also important when one considers a recently proposed scaling law for water in nanoconfined geometries. The self-diffusion coefficient of confined water was recently described as a linear combination of the diffusion coefficients of tightly confined and bulk water,[79] depending only on the ratio between the volumes of the two water populations. While a useful approach, it is somewhat inappropriate without a defined length scale of the measurement. It would be more satisfying if the framework took into account the different q dependencies of hydration and bulk water dynamics, which play a crucial role at nanometer length scales.

In summary, we have presented an experimentally determined picture of hydration water in a 100 mg/mL solution of GFP. This study utilized two-dimensional NS data, presented as the dynamic susceptibility stitched across multiple spectrometers at constant wavevector. This method allows researchers to analyze data over an extended dynamic range as a function of q, and its wider adoption may benefit other studies. We observed that just under two full shells (5.5 Å) of water were affected by the protein (∼1470 water molecules). The motions of hydration water showed a substantial slowdown in their dynamics, with ξ of ∼4−10 in the first shell and ∼2−5 for perturbed waters in the second shell. This picture of hydration water is meant to inform a wide range of audiences such as the food science, personal care, and pharmaceutical industries, as well as scientific interests such as protein folding, binding, and recognition. We also note the systematic decrease of ξ as a function of q, highlighting the crucial influence of the probe length on the observed retardation factor of hydration water. This implies that the probe length (and/or the distribution of probe lengths) should always be taken into consideration when comparing results from different techniques. It is our hope that these observations will facilitate a better understanding within the diverse scientific and industrial communities interested in hydration water.

■ ASSOCIATED CONTENT

Supporting Information

One supporting table, and six supporting figures can be found in the Supporting Information The Supporting Information is available free of charge on the ACS Publications website at DOI: 10.1021/jacs.6b08845.

Detailed methods, table of incoherent and coherent scattering contributions, fitting statistics from SANS, results from DAMMIN algorithm, translational−rotational decoupling approximation, NS data at 303 K, comparisons of NS spectra at 280 and 303 K, and hydration water relaxation times with the two modeling methods (PDF)

■ AUTHOR INFORMATION

Corresponding Authors

*perticarolis@ornl.gov
*nickelsjd@ornl.gov

Author Contributions

¶S.P. and J.D.N. contributed equally.

Notes

The authors declare no competing financial interest.

■ ACKNOWLEDGMENTS

We acknowledge Brad O'Dell for assistance with Figure 1C and Rhonda Moody, Rick Goyette, and Carrie Gao for technical assistance. H.O'N. and Q.Z. acknowledge the support of the Center for Structural Molecular Biology funded by the DOE Office of Biological and Environmental Research under Contract FWP ERKP291. Research at Oak Ridge National Laboratory's Spallation Neutron Source was sponsored by the Scientific User Facilities Division, Office of Basic Energy Sciences, DOE. Oak Ridge National Laboratory facilities are sponsored by UT-Battelle, LLC, for the U.S. Department of Energy under Contract No. DEAC0500OR22725. Cover image credit/Genevieve Martin, ORNL.

■ REFERENCES

(1) Berendsen, H. J.; Postma, J. P.; van Gunsteren, W. F.; Hermans, J. *Intermolecular forces*; Springer: The Netherlands, 1981; p 331.
(2) Rupley, J. A.; Careri, G. *Adv. Protein Chem.* **1991**, *41*, 37.
(3) Fenimore, P. W.; Frauenfelder, H.; McMahon, B. H.; Parak, F. G. *Proc. Natl. Acad. Sci. U. S. A.* **2002**, *99*, 16047.
(4) Nickels, J. D.; Katsaras, J. *Membrane Hydration*; Springer International Publishing: Switzerland, 2015; p 45.
(5) Pal, S. K.; Zewail, A. H. *Chem. Rev.* **2004**, *104*, 2099.
(6) Ball, P. *Chem. Rev.* **2008**, *108*, 74.
(7) Levy, Y.; Onuchic, J. N. *Annu. Rev. Biophys. Biomol. Struct.* **2006**, *35*, 389.
(8) Toppozini, L.; Roosen-Runge, F.; Bewley, R. I.; Dalgliesh, R. M.; Perring, T.; Seydel, T.; Glyde, H. R.; Sakai, V. G.; Rheinstädter, M. C. *Soft Matter* **2015**, *11*, 8354.
(9) Asghar, A.; Henrickson, R. *Adv. Food Res.* **1982**, *28*, 231.
(10) Conti Nibali, V.; Havenith, M. *J. Am. Chem. Soc.* **2014**, *136*, 12800.
(11) Dellerue, S.; Bellissent-Funel, M.-C. *Chem. Phys.* **2000**, *258*, 315.
(12) Denisov, V. P.; Halle, B. *Faraday Discuss.* **1996**, *103*, 227.
(13) Fogarty, A. C.; Laage, D. *J. Phys. Chem. B* **2014**, *118*, 7715.
(14) Marchi, M.; Sterpone, F.; Ceccarelli, M. *J. Am. Chem. Soc.* **2002**, *124*, 6787.
(15) Nickels, J. D.; Atkinson, J.; Papp-Szabo, E.; Stanley, C.; Diallo, S. O.; Perticaroli, S.; Baylis, B.; Mahon, P.; Ehlers, G.; Katsaras, J.; Dutcher, J. R. *Biomacromolecules* **2016**, *17*, 735.
(16) Nickels, J. D.; O'Neill, H.; Hong, L.; Tyagi, M.; Ehlers, G.; Weiss, K. L.; Zhang, Q.; Yi, Z.; Mamontov, E.; Smith, J. C.; Sokolov, A. P. *Biophys. J.* **2012**, *103*, 1566.
(17) Pal, S. K.; Peon, J.; Zewail, A. H. *Proc. Natl. Acad. Sci. U. S. A.* **2002**, *99*, 1763.
(18) Perticaroli, S.; Comez, L.; Paolantoni, M.; Sassi, P.; Lupi, L.; Fioretto, D.; Paciaroni, A.; Morresi, A. *J. Phys. Chem. B* **2010**, *114*, 8262.
(19) Perticaroli, S.; Comez, L.; Paolantoni, M.; Sassi, P.; Morresi, A.; Fioretto, D. *J. Am. Chem. Soc.* **2011**, *133*, 12063.
(20) Russo, D.; Hura, G.; Head-Gordon, T. *Biophys. J.* **2004**, *86*, 1852.
(21) Settles, M.; Doster, W. *Faraday Discuss.* **1996**, *103*, 269.
(22) Steinhoff, H.-J.; Kramm, B.; Hess, G.; Owerdieck, C.; Redhardt, A. *Biophys. J.* **1993**, *65*, 1486.
(23) Sterpone, F.; Stirnemann, G.; Laage, D. *J. Am. Chem. Soc.* **2012**, *134*, 4116.

DOI: 10.1021/jacs.6b08845
J. Am. Chem. Soc. 2017, 139, 1098−1105

(24) Perticaroli, S.; Nakanishi, M.; Pashkovski, E.; Sokolov, A. P. *J. Phys. Chem. B* **2013**, *117*, 7729.
(25) Berne, B.; Harp, G. *Advances in chemical physics* **1970**, *17*, 63.
(26) Abseher, R.; Schreiber, H.; Steinhauser, O. *Proteins: Struct., Funct., Genet.* **1996**, *25*, 366.
(27) Qin, Y.; Wang, L.; Zhong, D. *Proc. Natl. Acad. Sci. U. S. A.* **2016**, *113*, 8424.
(28) Bée, M. *Quasielastic Neutron Scattering: principles and applications in solid state chemistry, biology and material science*; Adam Hilger, Bristol, UK, 1988.
(29) Comez, L.; Paolantoni, M.; Sassi, P.; Corezzi, S.; Morresi, A.; Fioretto, D. *Soft Matter* **2016**, *12*, 5501.
(30) Persson, E.; Halle, B. *Proc. Natl. Acad. Sci. U. S. A.* **2008**, *105*, 6266.
(31) Martinez, N.; Michoud, G.; Cario, A.; Ollivier, J.; Franzetti, B.; Jebbar, M.; Oger, P.; Peters, J. *Sci. Rep.* **2016**, *6*, 32816.
(32) Zhou, H.-X.; Bilsel, O. *Biophys. J.* **2014**, *106*, 771.
(33) Chalfie, M.; Kain, S. R. *Green Fluorescent Protein: Properties, Applications and Protocols*; John Wiley & Sons: Hoboken, NJ, 2005; Vol. *47*.
(34) Zhao, J. K.; Gao, C. Y.; Liu, D. *J. Appl. Crystallogr.* **2010**, *43*, 1068.
(35) Kim, H. S.; Martel, A.; Girard, E.; Moulin, M.; Härtlein, M.; Madern, D.; Blackledge, M.; Franzetti, B.; Gabel, F. *Biophys. J.* **2016**, *110*, 2185.
(36) SasView for Small Angle Scattering Analysis, http://www.sasview.org/.
(37) Mamontov, E.; Herwig, K. W. *Rev. Sci. Instrum.* **2011**, *82*, 085109.
(38) Ehlers, G.; Podlesnyak, A. A.; Niedziela, J. L.; Iverson, E. B.; Sokol, P. E. *Rev. Sci. Instrum.* **2011**, *82*, 085108.
(39) Schober, H. *J. Neutron Res.* **2014**, *17*, 109.
(40) Doster, W.; Cusack, S.; Petry, W. *Phys. Rev. Lett.* **1990**, *65*, 1080.
(41) Paciaroni, A.; Cornicchi, E.; Marconi, M.; Orecchini, A.; Petrillo, C.; Haertlein, M.; Moulin, M.; Sacchetti, F. *J. R. Soc., Interface* **2009**, *6*, S635.
(42) Roh, J.; Curtis, J.; Azzam, S.; Novikov, V.; Peral, I.; Chowdhuri, Z.; Gregory, R.; Sokolov, A. *Biophys. J.* **2006**, *91*, 2573.
(43) Teixeira, J.; Bellissent-Funel, M.-C.; Chen, S.-H.; Dianoux, A.-J. *Phys. Rev. A: At., Mol., Opt. Phys.* **1985**, *31*, 1913.
(44) Amann-Winkel, K.; Bellissent-Funel, M.-C.; Bove, L. E.; Loerting, T.; Nilsson, A.; Paciaroni, A.; Schlesinger, D.; Skinner, L. *Chem. Rev.* **2016**, *116*, 7570.
(45) Bellissent-Funel, M.; Teixeira, J.; Chen, S.; Dorner, B.; Middendorf, H.; Crespi, H. *Biophys. J.* **1989**, *56*, 713.
(46) Orecchini, A.; Paciaroni, A.; Francesco, A. D.; Petrillo, C.; Sacchetti, F. *J. Am. Chem. Soc.* **2009**, *131*, 4664.
(47) Sacchetti, F.; Suck, J.-B.; Petrillo, C.; Dorner, B. *Phys. Rev. E* **2004**, *69*, 061203.
(48) Tarek, M.; Tobias, D. *Phys. Rev. Lett.* **2002**, *88*, 138101.
(49) Di Cola, D.; Deriu, A.; Sampoli, M.; Torcini, A. *J. Chem. Phys.* **1996**, *104*, 4223.
(50) Liu, L.; Faraone, A.; Mou, C.; Yen, C.; Chen, S. *J. Phys.: Condens. Matter* **2004**, *16*, S5403.
(51) Perticaroli, S.; Ehlers, G.; Jalarvo, N.; Katsaras, J.; Nickels, J. D. *J. Phys. Chem. Lett.* **2015**, *6*, 4018.
(52) Perticaroli, S.; Nickels, J. D.; Ehlers, G.; O'Neill, H.; Zhang, Q.; Sokolov, A. P. *Soft Matter* **2013**, *9*, 9548.
(53) Perticaroli, S.; Nickels, J. D.; Ehlers, G.; Sokolov, A. P. *Biophys. J.* **2014**, *106*, 2667.
(54) Nickels, J. D.; Perticaroli, S.; O'Neill, H.; Zhang, Q.; Ehlers, G.; Sokolov, A. P. *Biophys. J.* **2013**, *105*, 2182.
(55) Haupts, U.; Maiti, S.; Schwille, P.; Webb, W. W. *Proc. Natl. Acad. Sci. U. S. A.* **1998**, *95*, 13573.
(56) Nickels, J. D.; Garcia-Sakai, V.; Sokolov, A. P. *J. Phys. Chem. B* **2013**, *117*, 11548.
(57) Roosen-Runge, F.; Hennig, M.; Zhang, F.; Jacobs, R. M. J.; Sztucki, M.; Schober, H.; Seydel, T.; Schreiber, F. *Proc. Natl. Acad. Sci. U. S. A.* **2011**, *108*, 11815.
(58) Grimaldo, M.; Roosen-Runge, F.; Zhang, F.; Seydel, T.; Schreiber, F. *J. Phys. Chem. B* **2014**, *118*, 7203.
(59) Stingaciu, L. R.; Ivanova, O.; Ohl, M.; Biehl, R.; Richter, D. *Sci. Rep.* **2016**, *6*, 22148.
(60) Grimaldo, M.; Roosen-Runge, F.; Hennig, M.; Zanini, F.; Zhang, F.; Zamponi, M.; Jalarvo, N.; Schreiber, F.; Seydel, T. *J. Phys. Chem. Lett.* **2015**, *6*, 2577.
(61) Roos, M.; Ott, M.; Hofmann, M.; Link, S.; Rössler, E.; Balbach, J.; Krushelnitsky, A.; Saalwächter, K. *J. Am. Chem. Soc.* **2016**, *138*, 10365.
(62) Perticaroli, S.; Russo, D.; Paolantoni, M.; Gonzalez, M.; Sassi, P.; Nickels, J.; Ehlers, G.; Comez, L.; Pellegrini, E.; Fioretto, D.; Morresi, A. *Phys. Chem. Chem. Phys.* **2015**, *17*, 11423.
(63) Bahar, I.; Lezon, T. R.; Yang, L.-W.; Eyal, E. *Annu. Rev. Biophys.* **2010**, *39*, 23.
(64) Pontecorvo, E.; Krisch, M.; Cunsolo, A.; Monaco, G.; Mermet, A.; Verbeni, R.; Sette, F.; Ruocco, G. *Phys. Rev. E* **2005**, *71*, 011501.
(65) Phillips, J. C.; Braun, R.; Wang, W.; Gumbart, J.; Tajkhorshid, E.; Villa, E.; Chipot, C.; Skeel, R. D.; Kale, L.; Schulten, K. *J. Comput. Chem.* **2005**, *26*, 1781.
(66) MacKerell, A. D., Jr; Bashford, D.; Bellott, M.; Dunbrack, R. L., Jr; Evanseck, J. D.; Field, M. J.; Fischer, S.; Gao, J.; Guo, H.; Ha, S.; et al. *J. Phys. Chem. B* **1998**, *102*, 3586.
(67) Chen, X.; Weber, I.; Harrison, R. W. *J. Phys. Chem. B* **2008**, *112*, 12073.
(68) Lounnas, V.; Pettitt, B.; Phillips, G., Jr *Biophys. J.* **1994**, *66*, 601.
(69) Wong, C. F.; Andrew McCammon, J. *Isr. J. Chem.* **1986**, *27*, 211.
(70) Kuntz, I. D.; Kauzmann, W. *Adv. Protein Chem.* **1974**, *28*, 239.
(71) Rupley, J. A.; Gratton, E.; Careri, G. *Trends Biochem. Sci.* **1983**, *8*, 18.
(72) Schirò, G.; Fichou, Y.; Gallat, F.-X.; Wood, K.; Gabel, F.; Moulin, M.; Härtlein, M.; Heyden, M.; Colletier, J.-P.; Orecchini, A.; et al. *Nat. Commun.* **2015**, *6*, 6490.
(73) Volino, F.; Dianoux, A. *Mol. Phys.* **1980**, *41*, 271.
(74) Combet, S.; Zanotti, J.-M. *Phys. Chem. Chem. Phys.* **2012**, *14*, 4927.
(75) Hong, L.; Smolin, N.; Lindner, B.; Sokolov, A. P.; Smith, J. C. *Phys. Rev. Lett.* **2011**, *107*, 148102.
(76) Rocchi, C.; Bizzarri, A. R.; Cannistraro, S. *Phys. Rev. E: Stat. Phys., Plasmas, Fluids, Relat. Interdiscip. Top.* **1998**, *57*, 3315.
(77) Stirnemann, G.; Sterpone, F.; Laage, D. *J. Phys. Chem. B* **2011**, *115*, 3254.
(78) Stirnemann, G.; Wernersson, E.; Jungwirth, P.; Laage, D. *J. Am. Chem. Soc.* **2013**, *135*, 11824.
(79) Chiavazzo, E.; Fasano, M.; Asinari, P.; Decuzzi, P. *Nat. Commun.* **2014**, *5*, 4565.

DOI: 10.1021/jacs.6b08845
J. Am. Chem. Soc. 2017, 139, 1098−1105